03

Oscillations of a suspended cylinder with stabilizer in the air flow

© A.N. Ryabinin, M.I. Ivanov, A.V. Danilov

St. Petersburg State University,
St. Petersburg, Russia
e-mail: a.ryabinin@spbu.ru

Received June 24, 2025
Revised November 9, 2025
Accepted November 25, 2025

In experiments in a wind tunnel, the oscillations of a circular cylinder equipped with a stabilizer are studied. The cylinder is suspended in the air stream by a cable suspension and can oscillate. The axis of the cylinder in the equilibrium position is directed at a slight negative angle of attack to the direction of the incoming flow velocity. The stabilizer holds the cylinder in this position, providing low drag. The oscillations of the cylinder in the air flow are recorded by the accelerometer, which, together with the controller, is located inside the cylinder. The device makes it possible to measure three projections of the angular velocity of the cylinder on the axis of the coordinate system associated with the cylinder. In a separate experiment, the aerodynamic coefficients of forces and moments acting on the cylinder are determined. The mathematical model previously proposed for describing cylinder oscillations has been modified. The model correctly describes the angular oscillations of the cylinder around an axis close to the vertical, transverse vibrations, the amplitude of which increases with increasing air flow velocity, and the beating mode that occurs in a certain range of air flow velocities.

Keywords: wind tunnel, accelerometer, bluff body, mathematical model, ordinary differential equations, similarity numbers.

DOI: 10.61011/TP.2026.03.63155.162-25

Introduction

Unacceptable swings, which potentially lead to accidents, may occur when poorly streamlined bodies are transported as a sling load. Specifically, these situations arise when cargo is suspended underneath an aircraft (e.g., a helicopter) [1].

S.V. Siparov has examined the stability of a sling load underneath a helicopter [2]. He has obtained a characteristic equation intended for analyzing the stability of load motion. The Routh–Hurwitz criterion was proposed as a means to determine stability, which was defined as the lack of motion of the suspended load relative to the suspension point. From a safety standpoint, this requirement is excessive. Oscillations posing no danger to the aircraft are permissible. The equations of motion of a load secured underneath a helicopter with a two-link suspension were considered in [3]; it was assumed that the helicopter does, in the general case, move along a curved trajectory with varying speed. A system of ordinary differential equations of the 24th order was obtained. An example of calculations for the motion of a helicopter transporting a container was provided. The dependences of aerodynamic forces for the load on angles characterizing its orientation were not discussed. A generalized approach to modeling the motion of a helicopter with a sling load was presented in [4]. However, as before, no attention was paid to the specific type of aerodynamic forces. A large amount of data regarding sling loads were provided in monograph [5]. Devices used to stabilize the motion of cargo suspended underneath a helicopter, the construction of equations of motion, and the coordinate systems used for this purpose were discussed.

The model of interaction between a load suspended on a cable and a helicopter was considered in [6] with the accelerated motion of the cable suspension point to the helicopter taken into account. The specific type of aerodynamic forces was left unaddressed. A comparison of data obtained in a wind tunnel experiment and through calculations with a mathematical model was performed in [7]. A mode of oscillation with a constant amplitude and a beating mode were reported.

Study [8] was focused on the analysis of motion of a cylindrical load with ratio $\lambda = L/D = 2$ between length L and diameter D. The load was assumed to be suspended on a cable underneath a helicopter and transported at a constant speed. The load had a stabilizer; when in equilibrium, it positioned the cylinder in the direction corresponding to minimum drag. However, this position was unstable. The cylinder underwent angular oscillations around a vertical axis. Angular oscillations do not pose a flight hazard if their frequency differs significantly from the frequency of oscillations of the suspended load under the force of gravity. Close frequencies lead to resonance phenomena, which induce intense and dangerous transverse oscillations of the load. In the mathematical model proposed in [8], the aerodynamic coefficients of crosswind force and yaw moment are represented as linear functions of the sideslip angle, and angular oscillations around the vertical

axis are characterized by a differential equation of the van der Pol type.

In the present study, we examine experimentally the oscillations of a cylinder with a stabilizer. The mathematical model proposed in [8] is modified.

One common method for studying oscillations is the remote determination of the position of a moving body by a triangulation laser displacement sensor. Such sensors are used mainly to examine the oscillations of bodies in one direction [9,10]. Another method is to use strain gauges in the elastic suspension of an oscillating body [11,12]. Both of these techniques are hard to implement in an experiment on oscillations of a body suspended in a flow. Accelerometers are the best suited for this scenario and provide ample opportunities when coupled with an Arduino controller. This controller has become ubiquitous due to the wide-scale development of robotics. It may act as a link between dozens of sensors of various physical quantities and computers. The increase in popularity and production volumes has led to a significant reduction in cost of such devices. Controllers developed by the Italian company Arduino are manufactured in many countries under different names, which is permitted by the developer. Arduino controllers coupled with accelerometers are used to determine the angles characterizing the orientation of various types of aircraft. Specifically, an Arduino controller with accelerometers is used in aircraft-type unmanned aerial vehicles and quadcopters [13,14].

This method of recording the motion of a body suspended in air flow was chosen in the present study.

1. Experimental determination of the projections of angular velocity onto the axes of a bound coordinate system

Experiments were carried out in the AT-12 wind tunnel of St. Petersburg State University [15]. The wind tunnel has an open working section; the nozzle exit section is a circle 1.5 m in diameter. The air flow velocity may be adjusted smoothly within the range from 0 to 40 m/s.

Figure 1 presents the schematic diagram of an experiment with the cylinder suspended in the working section of the wind tunnel. The distance from the suspension point to the cylinder axis is $l = 1.06$ m, cylinder length $L = 0.46$ m, and cylinder diameter $D = 0.25$ m. A stabilizer (flat rectangular plate) is secured rigidly to the aft body of the cylinder. The length of the stabilizer is 0.21 m, and its height is 0.115 m. Thus, the area of the stabilizer is two times smaller than the cross-sectional area of the cylinder. The suspension arrangement is made of cotton thread. With zero air flow, the cylinder is positioned at the center of the working section.

A GY-521 accelerometer based on an MPU 6050 microcircuit and a Piranha UNO controller, which is an improved

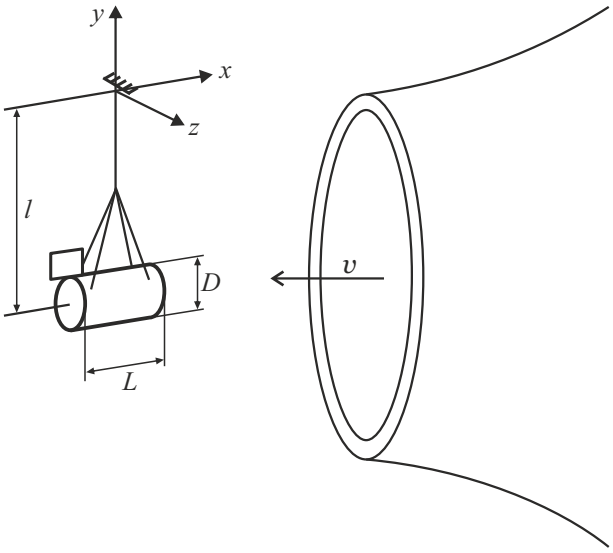

Figure 1. Diagram of the experiment.

alternative to Arduino UNO, are positioned in a cavity at the center of the cylinder.

The GY-521 accelerometer measures three projections of acceleration acting on the body onto the axes of a non-inertial coordinate system bound rigidly to the microcircuit and, consequently, to the cylinder. If the device is stationary, the projection onto the vertical axis is equal to unity. In addition, the accelerometer includes three gyroscopes that measure three projections of angular velocity onto the same axes. The freeware Arduino integrated development environment (IDE) is used to program the controller and take readings. The controller is connected to a computer by a shielded cable 6 m in length. A version of C is used for programming. The Arduino IDE establishes a virtual serial port through which code is uploaded from the computer to the controller and data are read out from the controller. A small program was written in Free Pascal in order to process the measurement data. It transfers data from the serial port to a text file. Data in text files were processed further. Each file contained 1700 lines with data read from six channels and the readout time in each line. The data readout interval was $\Delta t = 0.017$ s.

The accelerometer was calibrated in order to determine the coefficients relating the instrument readings to the angular velocity projections. The results of measurement of acceleration and angular velocity during cylinder oscillations with zero air flow in the working section of the wind tunnel were used for calibration. The division value for acceleration readings was determined in one of the channels where the projection onto the vertical axis of the stationary cylinder was recorded. The cylinder was then swung in a plane containing the suspension point and the cylinder axis. These oscillations decayed slowly. The maximum and minimum acceleration readings and the oscillation period were determined based on the periodically

changing readings in the same channel, and the amplitude of angular oscillations was then calculated. Owing to their small amplitude, the oscillations were regarded as harmonic, and the angular velocity was calculated as a function of time. The angular velocity measurement channel did also record the dependence of angular velocity on time. A comparison of the readings in two channels was the basis for determining the calibration coefficient relating the readings of the angular velocity measurement channel to true angular velocity values. The linearity was evaluated by repeating measurements multiple times at different oscillation amplitudes. The variation of sensitivity was determined by rotating the accelerometer by an angle of π. It turned out that the device readings may differ slightly when the direction of the axis is changed. The manufacturer did not specify the error in determining the angular velocity. Therefore, the error had to be estimated based on the calibration results. It does not exceed 3 % of the full scale value, which is $4.4\,\mathrm{s}^{-1}$.

2. Mathematical model of oscillations of a cylinder with a stabilizer in air flow

It is assumed that the suspension links are inextensible and do not transmit torque. Aerodynamic forces acting on the suspension links are neglected. The suspension with the cylinder is a two-link pendulum oscillating with five degrees of freedom. However, since the cylinder in experiments moved with three degrees of freedom only, the mathematical model is limited to such motion. Let us assume that the suspension point moves with a constant velocity and this point is the origin of the bound coordinate system. Axes x, y, and z of the orthogonal coordinate system are parallel to the principal axes of inertia of the cylinder with the stabilizer. The axes are indicated in Fig. 1. Longitudinal axis x is directed parallel to the cylinder axis from the aft body to the fore body. Normal axis y is positioned in the plane of symmetry of the cylinder with the stabilizer and directed upward along the suspension axis. Transverse axis z forms a right-hand system with axes x and y. The cylinder position is characterized by angles γ, ϑ, and ψ. They are denoted in the same way as the roll, pitch, and yaw angles used in flight dynamics [16]. Successive rotations by these angles translate axes x_g, y_g, and z_g of the normal coordinate system into the axes of the bound coordinate system. The origin of the normal moving coordinate system is also located at the suspension point. Axis x_g is directed horizontally along the velocity vector of the suspension point relative to the environment, axis y_g is directed upward, and z_g forms a right-hand orthogonal coordinate system with the first two axes. The first rotation by γ around axis x_g translates axes y_g and z_g into axes y'_g and z'_g. The second rotation by ϑ is performed around axis z'_g. It translates axis y'_g into axis y. The third rotation around axis y by ψ completes the translation of the normal coordinate system into the bound one. Small angles γ, ϑ, and ψ match the roll, pitch, and yaw angles defined in [16].

We define the aerodynamic forces in the velocity coordinate system x_a, y_a, z_a, which is translated into the bound one by two successive rotations by angles α and β. The angle designations are the same as the angle of attack and sideslip angle designations established by standard [16], but the order of rotations is changed. At small angles, the indicated angles match the angle of attack and the sideslip angle. In the velocity coordinate system, axis x_a is directed along the velocity vector of the cylinder center relative to the environment, axis y_a lies in the plane of symmetry of the cylinder with the stabilizer and is directed toward the upper part of the cylinder, and axis z_a forms a right-hand system with the first two.

The first rotation by α is performed around axis z_a. It translates axis y_a into axis y. The second rotation around the y axis by angle β completes the transition from the velocity coordinate system to the bound one.

The equations of motion of the cylinder in projections onto the axes of the bound rotating coordinate system are written as [17]

$$\begin{aligned} J_x\dot{\omega}_x - (J_y - J_z)\omega_y\omega_z &= L_x,\\ J_y\dot{\omega}_y - (J_z - J_x)\omega_z\omega_x &= L_y,\\ J_z\dot{\omega}_z - (J_x - J_y)\omega_x\omega_y &= L_z, \end{aligned} \tag{1}$$

where $\omega_x, \omega_y, \omega_z$ are the projections of angular velocity on axes x, y, z; J_x, J_y, J_z are the elements of the diagonal inertia tensor; and L_x, L_y, L_z are the projections of the moment of force acting on the cylinder relative to the suspension point. The next simplifying assumption is that the moment of inertia of the cylinder relative to its own center of mass is neglected in comparison with the moment of inertia relative to the suspension point: $J_x \approx J_z >> J_y$. The projections of angular velocity are expressed in terms of roll, pitch, and yaw angles:

$$\begin{aligned} \omega_x &= \dot{\vartheta}\sin\psi + \dot{\gamma}\cos\psi\cos\vartheta,\\ \omega_y &= \dot{\psi} - \dot{\gamma}\sin\vartheta,\\ \omega_z &= \dot{\vartheta}\cos\psi + \dot{\gamma}\sin\psi\cos\vartheta. \end{aligned} \tag{2}$$

With the projections of angular velocity and their derivatives inserted into system (1), it takes the form

$$\begin{aligned} \ddot{\vartheta} &= -\dot{\gamma}^2\sin\vartheta\cos\vartheta + (\cos\psi L_z - \sin\psi L_x)/J_z,\\ \ddot{\gamma} &= 2\dot{\gamma}\dot{\vartheta}\sin\vartheta + (\sin\psi L_z + \cos\psi L_x)/J_z,\\ \ddot{\psi} &= \ddot{\gamma}\sin\vartheta + \dot{\gamma}\dot{\vartheta}\cos\vartheta + L_y/J_x. \end{aligned} \tag{3}$$

The projections of moment of forces L_x, L_y, and L_z on the axes of the bound coordinate system are given by

$$L_x = -F_z l, \quad L_y = L'_y, \quad L_z = -F_x l,$$

where F_x is the projection of force acting on the cylinder onto the longitudinal axis (with the opposite sign) and F_z is

the projection of force onto the transverse axis of the bound coordinate system. F_x and F_z are the sums of projections of the gravity force and the aerodynamic force. L'_y is the projection of moment of forces relative to the center of mass of the cylinder onto axis y.

To obtain the equations of motion in projections onto the axes of the bound coordinate system, one needs to transform the projections of aerodynamic force from projections onto the axes of the velocity coordinate system. The projections of gravity force from the normal coordinate system must be converted into projections of the bound coordinate system. The projections of aerodynamic force onto axes X_a, Y_a, and Z_a of the velocity coordinate system are expressed in terms of the aerodynamic coefficients of drag c_{xa}, lift c_{ya}, and crosswind force c_{za}:

$$X_a = c_{xa} qs, \quad Y_a = c_{ya} qs, \quad Z_a = c_{za} qs,$$

where s is the cross-sectional area of the cylinder; $q = \rho u^2/2$ is the velocity pressure; ρ is the air density; and u is the velocity of the cylinder center relative to the environment. The projection onto the velocity axis, which is called the drag, is also taken with the opposite sign [16].

The vector of projections of aerodynamic force in the bound coordinate system X, Y, and Z is found by multiplying the transformation matrix by a vector with its elements being the projections of aerodynamic force in the velocity coordinate system:

$$\begin{pmatrix} X \\ Y \\ Z \end{pmatrix} = \begin{pmatrix} \cos\beta\cos\alpha & \cos\beta\sin\alpha & -\sin\beta \\ -\sin\alpha & \cos\alpha & 0 \\ \sin\beta\cos\alpha & \sin\beta\sin\alpha & \cos\beta \end{pmatrix} \begin{pmatrix} X_a \\ Y_a \\ Z_a \end{pmatrix}.$$

The vector of force projections in the bound coordinate system is equal to the sum of the vector of aerodynamic forces and the vector of gravity force projections: $F_x = X + P_x$, $F_y = Y + P_y$, and $F_z = Z + P_z$. The vector of gravity force projections has only one nonzero projection in the normal coordinate system:

$$\begin{pmatrix} -P_x \\ P_y \\ P_z \end{pmatrix} = \begin{pmatrix} \cos\psi\cos\vartheta & \cos\psi\sin\vartheta\cos\gamma + \\ & +\sin\psi\sin\gamma \\ \sin\vartheta & \cos\vartheta\cos\gamma \\ \sin\psi\cos\vartheta & \sin\psi\sin\vartheta\cos\gamma - \\ & -\cos\psi\sin\gamma \end{pmatrix} \begin{matrix} \cos\psi\sin\vartheta\sin\gamma - \\ -\sin\psi\cos\gamma \\ \cos\vartheta\sin\gamma \\ \sin\psi\sin\vartheta\sin\gamma + \\ \cos\psi\cos\gamma \end{matrix} \times \begin{pmatrix} 0 \\ -mg \\ 0 \end{pmatrix},$$

where m is the cylinder mass and g is the gravitational acceleration. There is a minus sign in front of P_x, since the projection of gravity force onto the longitudinal axis is taken with the opposite sign.

To make the formulae more compact, we introduce the following notation: $\varepsilon = \psi - \beta$. The equations of motion then take the form

$$\begin{aligned} \ddot{\vartheta} &= -\dot{\gamma}^2 \sin\vartheta\cos\vartheta + qsl\Big(\cos\varepsilon(c_{xa}\cos\alpha + c_{ya}\sin\alpha) \\ &\quad + c_{za}\sin\varepsilon\Big)/J_z mgl\sin\vartheta\cos\gamma/J_z, \\ \ddot{\gamma}\cos\vartheta &= 2\dot{\gamma}\dot{\vartheta}\sin\vartheta + qsl\Big(\sin\varepsilon(c_{xa}\cos\alpha + c_{ya}\sin\alpha) \\ &\quad - c_{za}\cos\varepsilon\Big)/J_z mgl\sin\gamma/J_z, \\ \ddot{\psi} &= \ddot{\gamma}\sin\vartheta + \dot{\gamma}\dot{\vartheta}\cos\vartheta + qsL\left(m_y + L\dot{\beta}m_y^{\dot{\beta}}/v\right), \end{aligned} \tag{4}$$

where m_y and $m_y^{\dot{\beta}}$ are the yaw moment coefficient and the rotational derivative of yaw moment. The following expression for the rotational derivative for a cylinder has already been proposed [1]:

$$m_y^{\dot{\beta}} = \mu(1 - \delta\beta^2).$$

Expression (5) contains two parameters that specify the amplitude of rotational oscillations in yaw angle and the rate of its change. This form of the rotational derivative provides an opportunity to explain self-oscillations of a cylinder fixed elastically in gas flow. A simpler representation $\mu = \text{const}$ characterizes the decay of oscillations (if $\mu < 0$) or an unbounded increase in their amplitude (if $\mu > 0$). The presence of a second-order term in formula (5) leads to steady oscillations with a constant amplitude determined by parameter δ. The value of parameter δ may be estimated based on the amplitude of oscillations in yaw angle in the mode featuring no other types of oscillations. Experiments focused on examining the mode of oscillations in yaw angle were carried out in [18]. A wire suspension in these experiments allowed the cylinder with $L/D = 2$ to oscillate with just one degree of freedom. The cylinder had no stabilizer. The force returning the cylinder back to its equilibrium position was produced by steel springs. It was found that $\delta = 68$ in the case when the axis of rotation passes through the center of the cylinder. The introduction of a stabilizer alters this parameter. In addition, the frequency of oscillations of the spring-suspended cylinder was much higher than the oscillation frequency of the suspended cylinder.

The relations between angles ε, α, ϑ, and γ were obtained in [8]:

$$\tan\varepsilon = \frac{\dot{\gamma} l\cos\vartheta}{\dot{\vartheta} l + \cos\vartheta v}, \quad \tan\alpha = \frac{\cos\varepsilon\sin\vartheta v}{\dot{\vartheta} l + v\cos\vartheta}. \tag{6}$$

The relation between velocity v of the suspension point and relative velocity u of the center of mass of the cylinder and the environment under the condition of smallness of $l\dot{\vartheta}/v << 1$ and $l\dot{\gamma}/v << 1$ was also obtained in this study:

$$u^2 \approx v^2\left(1 + 2\cos\vartheta l\dot{\vartheta}/v\right). \tag{7}$$

At the next stage, the equations of motion are transformed under the assumption that angles ϑ, ψ, and γ and their derivatives are small. Expressions (6) are simplified:

$$\varepsilon = \frac{\dot{\gamma} l}{v}, \quad \alpha = \vartheta. \tag{8}$$

Only the angles raised to the first power are left in the equations of motion. The term with $\delta\beta^2$, which is on the order of unity, does also remain in place. Angle ψ is excluded from the equations.

The following considerations allow one to estimate the influence of motion of the stabilizer, which is secured rigidly to the aft body of the cylinder, and to introduce terms containing the time derivative of yaw angle ψ into the equations. Rotation of the stabilizer under the assumption of smallness of angle ψ results in a small additional change in sideslip angle of the stabilizer. Its velocity in the transverse direction differs from the velocity of the cylinder center by $\dot{\psi}(L/2)$. The ratio of the additional transverse velocity to the flow velocity is equal to the difference in sideslip angles at the centers of the stabilizer and the cylinder. Using the first formula in (8), one may express this angle difference in terms of derivatives of angles β and γ:

$$\Delta\psi = \dot{\psi}(L/2)/v = \dot{\beta}(L/2)/v + \ddot{\gamma} lL/(2v^2). \tag{9}$$

In this expression, $\ddot{\gamma}$ is substituted with the formula derived from the second equation in (4), where the aerodynamic force, which is small compared to the force of gravity, and the term on the right-hand side containing the product of two small derivatives of roll and pitch angles are neglected. The assumption of smallness of the aerodynamic force relative to the force of gravity is verified by the fact that oscillations in roll angle are nearly harmonic. The sine of a small roll angle is replaced by the angle itself, and the cosine of the pitch angle is replaced by unity. It is assumed that the coefficients of crosswind force c_s and stabilizer yaw moment m_s depend linearly on $\Delta\psi$:

$$c_s = -c_{zs}\Delta\psi, \; Z_s = c_s qs, \; m_s = -m_{ys}\Delta\psi, \; M_{ys} = m_s qsL,$$

where Z_s and M_{ys} are the crosswind force and the yaw moment acting on the stabilizer. Thus, equations of motion (4) are transformed to the form

$$\ddot{\vartheta} = rv^2\left(-c_{xa} + c_{za}\dot{\gamma}\frac{l}{v} - 2c_{xa}\dot{\vartheta}\frac{l}{v}\right) - \omega^2\vartheta,$$

$$\ddot{\gamma} = rv^2\left(-c_{xa}\dot{\gamma}\frac{l}{v} - c_{za} - c_{zs}\left(\dot{\beta}\frac{L}{2v} - \gamma\frac{lL\omega^2}{2v^2}\right)\right) - \omega^2\gamma,$$

$$\ddot{\beta} = r_1 v^2\left(m_y - \left(\dot{\beta}\frac{L}{2v} - \gamma\frac{lL\omega^2}{2v^2}\right) + \mu\frac{L}{v}(1-\delta\beta^2)\dot{\beta}\right) + \dot{\gamma}\frac{l}{v}\omega^2,$$

where $r = \rho s/(2ml)$; $r_1 = \rho sL/(2J_y)$; $\omega^2 = g/l$.

System (10) below represents the dimensionless equations of motion. Differentiation in them is performed with respect to dimensionless time $\tau = t\omega$, where t is actual time.

$$\ddot{\vartheta} + \vartheta = R\nu\left(-\nu c_{xa} + \dot{\gamma}c_{za} - 2c_{xa}\dot{\vartheta}\right),$$

$$\ddot{\gamma} + \gamma = R\nu\left(-\nu c_{za} - c_{xa}\dot{\gamma} - c_{zs}\left(\dot{\beta} - \frac{\gamma}{\nu}\right)\frac{L}{2l}\right), \tag{10}$$

$$\ddot{\beta} - R_1\nu^2 m_y = R_1\nu\left(-m_{ys}\left(\dot{\beta} - \frac{\gamma}{\nu}\right)\frac{L}{2l} + \mu\frac{L}{l}\dot{\beta}\left(1-\delta\beta^2\right)\right) + \frac{\dot{\gamma}}{\nu}.$$

The following notation is used in dimensionless equations of motion (10): $R = \rho sl/(2m)$; $R_1 = \rho sL l^2/(2J_y)$; $\nu = v/(l\omega) = v/\sqrt{gl}$. The equations of motion in dimensionless form allow one to write down the similarity numbers: ν is the dimensionless air flow velocity; $\rho sl/m$ is the quantity proportional to the ratio of air density and average density of the cylinder; l/L is the relative suspension length; and $J_y/(ml^2)$ is the similarity number that characterizes the distribution of density of the cylinder over its volume. Dimensionless flow velocity ν may be substituted with Strouhal number $\mathrm{Sh} = \omega l/(2\pi v)$, which is inversely proportional to ν, or treated as Froude number $Fr = v/\sqrt{gl}$. Since the aerodynamic coefficients found in the equations of motion may depend on the Reynolds number, it should also be included in the list of similarity numbers. If the similarity numbers are known, one may extend the results of physical and mathematical modeling to a set of objects characterized by the same similarity numbers.

It follows from system (10) that oscillations in pitch angle within the model do not affect oscillations in sideslip and roll angles.

Equations of motion (10) for the cylinder were solved by the fourth-order Runge–Kutta method.

3. Determination of aerodynamic coefficients

The equations of motion contain the aerodynamic coefficients of drag c_{xa}, crosswind force c_{za}, yaw moment of the cylinder with the stabilizer m_y, and coefficients c_{zs} and m_{ys}. In the general case, these coefficients depend on angle of attack α and sideslip angle β.

It was assumed in the oscillation model presented in [8] that the crosswind force coefficient and the yaw moment coefficient depend linearly on the sideslip angle, while the drag coefficient is constant or is related quadratically to the sideslip angle within the range of angles where oscillations occur.

In the present study, the dependences of c_{za} and m_y on angle β are assumed to be non-linear, and the dependence of c_{xa} on β is non-quadratic. The experimentally determined dependences on sideslip angle are approximated in the mathematical model by polynomials that varied from one

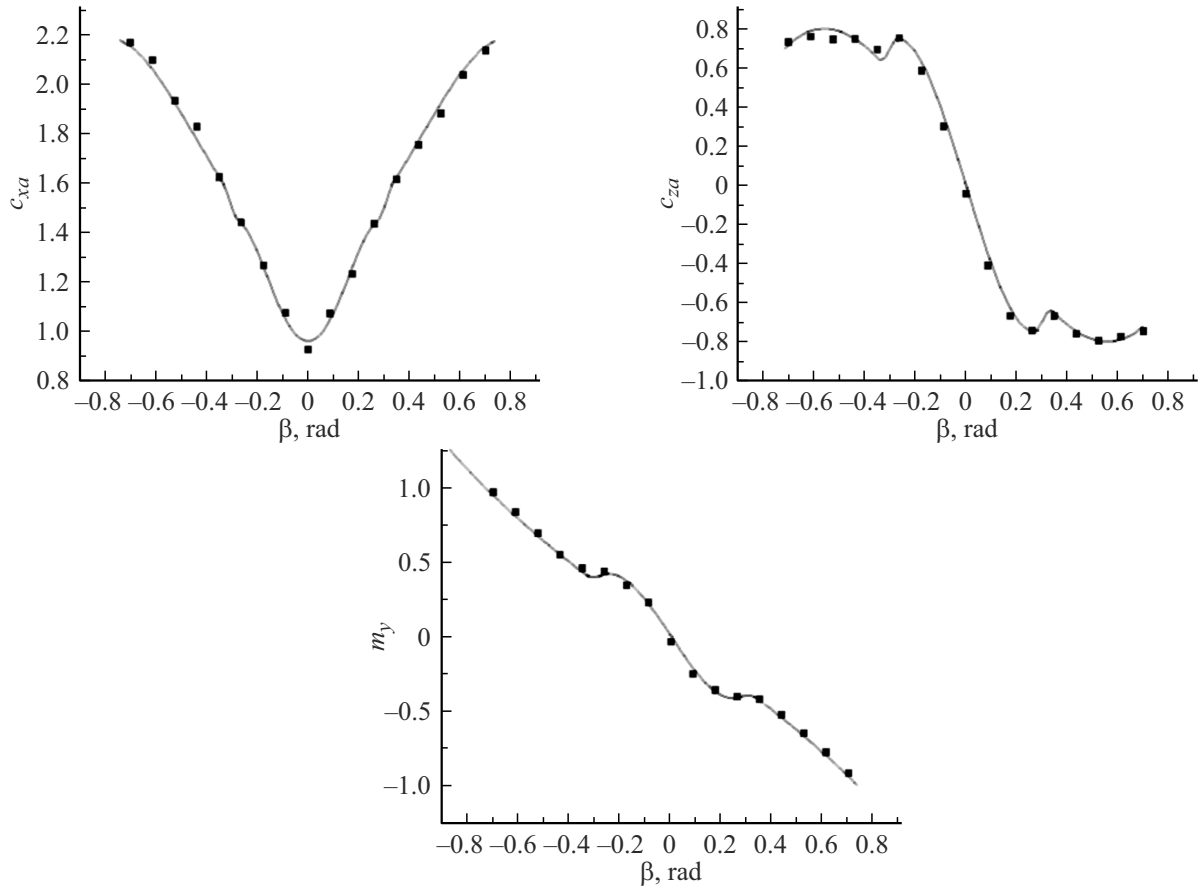

Figure 2. Aerodynamic coefficients of drag, crosswind force, and yaw moment as functions of sideslip angle β.

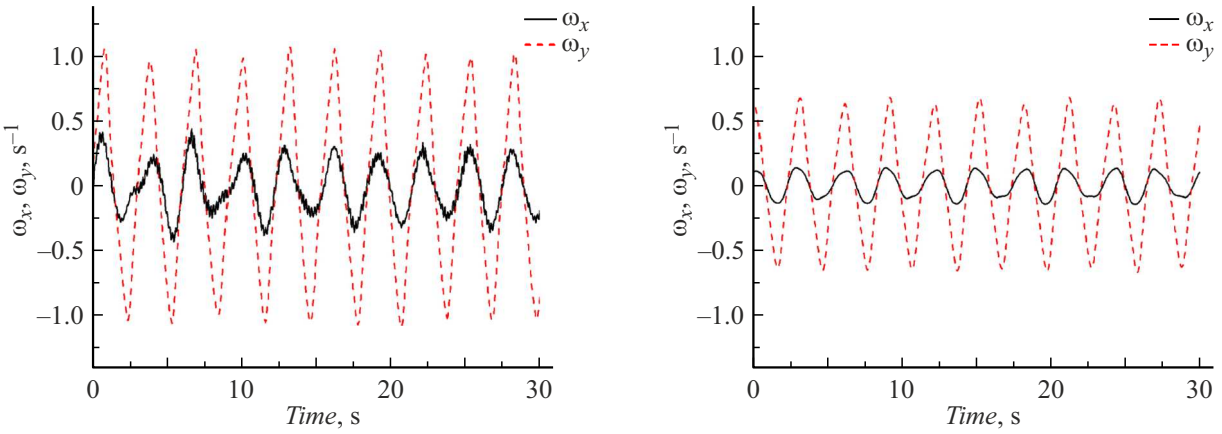

Figure 3. Rotational velocity components as functions of time. The oscillation amplitude remains roughly constant in this mode (v = 7.1 m/s, ν = 2.28). Experimental and calculated data are presented in the left and right panels, respectively.

range of sideslip angles to the other. Since the range of angles of attack is narrow, the dependence on angle of attack is neglected.

The aerodynamic coefficients of crosswind force and stabilizer yaw moment are assumed to depend linearly on yaw angle. It is hard to determine these coefficients experimentally with the cylinder present. Therefore, the values of c_{zs} and m_{ys} were chosen based on the data reported in [19] for a rectangular plate with an aspect ratio of two. The plots presented in [19] demonstrate that the lift coefficient of the plate depends linearly on angle of attack within the range from -0.17 to 0.17 rad, and the slope of the linear dependence is 4. We assumed that the characteristic area is equal not to the area of the stabilizer,

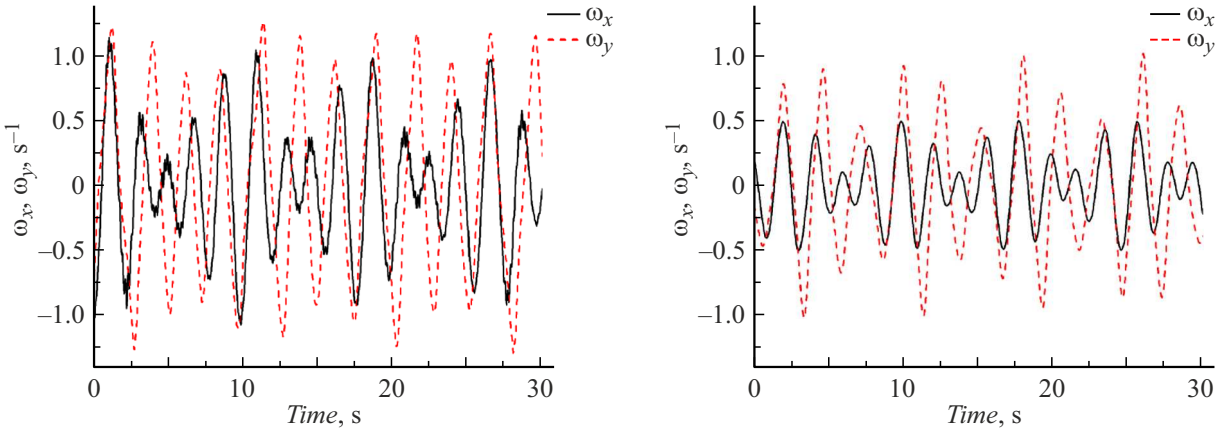

Figure 4. Angular velocity components as functions of time. The beating mode ($v = 8.1$ m/s, $\nu = 2.6$). Experimental and calculated data are presented in the left and right panels, respectively.

but to the cross-sectional area of the cylinder, which is twice as large; therefore, $c_{zs} = 2$. The moment of forces is equal to the lift force multiplied by arm $L/2$. With cylinder length L taken as the characteristic length, coefficient $m_{ys} = 1.0$.

Aerodynamic coefficients c_{xa}, c_{za}, and m_y were measured using a three-component balance with a wire suspension.

Figure 2 presents the dependences of aerodynamic coefficients of drag, crosswind force, and yaw moment on sideslip angle. Points in the plots represent experimental data. The aerodynamic balance allows one to measure aerodynamic coefficients with an error below 5%. Solid curves represent the approximation dependences. The entire range of sideslip angles is divided into five sub-ranges, and a low-order polynomial approximation was performed using the least-squares method in each sub-range. The values of coefficients and their derivatives with respect to sideslip angle matched at the boundaries of these sub-ranges.

If $|\beta| > 0.34$, the dependences of aerodynamic coefficients on sideslip angle are written as

$$c_{xa} = 1.303 + 2.93\beta^2 - 2.4\beta^4,$$

$$c_{za} = -2.148\beta + 2.3\beta^3,$$

$$m_y = -1.189\beta - 0.33\beta^3.$$

At $|\beta| < 0.27$:

$$c_{xa} = 0.962 + 12.1\beta^2 - 75\beta^4,$$

$$c_{za} = -4.187\beta + 19.5\beta^3,$$

$$m_y = -2.553\beta + 14.2\beta^3.$$

At $0.27 < \beta < 0.34$:

$$c_{xa} = 15.861 - 145\beta + 478\beta^2 - 514\beta^3,$$

$$c_{za} = 22.47 - 236\beta + 792\beta^2 - 877\beta^3,$$

$$m_y = 1.396 - 21.73\beta + 84.6\beta^2 - 107\beta^3.$$

At $-0.34 < \beta < -0.27$:

$$c_{xa} = 15.861 - 145\beta - 478\beta^2 + 514\beta^3,$$

$$c_{za} = -22.47 - 236\beta - 792\beta^2 - 877\beta^3,$$

$$m_y = -1.396 - 21.73\beta - 84.6\beta^2 - 107\beta^3.$$

We failed to conduct an experiment to determine coefficient μ. The build-up time of oscillations with a constant amplitude depends on the value of this coefficient. It was assumed that $\mu = 2$. Parameter δ in the equations of motion was chosen so that the flow velocity corresponding to the transition from constant-amplitude oscillations to the beating mode matched the experimental value. It was found that $\delta = 88$. The set of parameters of the equations of motion is not the only possible one. With parameter μ assuming a different value, the value of δ will also change.

4. Experimental results and their comparison with predictions of the mathematical model

The experiment revealed that angular oscillations of the cylinder in yaw angle emerge at low air flow velocities. Their frequency is determined by the yaw moment returning to the equilibrium position and the moment of inertia of the cylinder. The amplitude of rotational oscillations increases with oncoming flow velocity. When the frequency approaches the frequency of oscillations of the suspended cylinder as a physical pendulum, oscillations in roll angle arise. At a specific oncoming flow velocity, the amplitude of oscillations in roll angle becomes constant rapidly. The dependence of two components of angular velocity on time is shown in Fig. 3.

Beating is observed when the dimensionless velocity of oncoming flow increases further to 2.3. Figure 4 shows the dependence of two components of angular velocity on time in this oscillation mode.

Experiments with even higher levels of flow velocity had to be stopped, since the moving cylinder crossed the boundaries of the homogeneous flow core in the working section. The mathematical model predicted that the beating mode would persist at higher velocities. That said, the assumptions that the motion is characterized by oscillations with small angles of deviation from the equilibrium position, which were put forward when the equations of motion were derived, are incorrect.

The scenarios of oscillation evolution observed in physical and mathematical modeling match. However, the experimental and calculated results differ quantitatively. This may be attributed to the incompleteness of the mathematical model and numerous assumptions regarding the angles characterizing deviations from the equilibrium position. Despite its simplicity, the model does still predict the main features of the phenomenon.

Conclusion

An experimental method for examining the oscillations of a cylinder with a stabilizer suspended in air flow, which is based on the measurement of acceleration and angular velocity with an accelerometer, was tested. The accelerometer was coupled with an Arduino controller. Angular oscillations around the vertical axis were observed when the flow velocity increased. An increase in velocity led to the emergence of intense transverse oscillations with a constant amplitude. As the velocity increased further, oscillations entered the beating mode. A simple mathematical model, which has been proposed in earlier studies, was modified. The modified model characterizes correctly the evolution of oscillation modes with a change in air flow velocity. The mathematical model is a system of ordinary differential equations in dimensionless form. The similarity numbers of the phenomenon were determined.

Funding

This study was supported financially by St. Petersburg State University (project 128783603).

Conflict of interest

The authors declare that they have no conflict of interest.

References

[1] A.N. Ryabinin, B.F. Tyurin. Vestn. S.-Peterb. Univ. Ser. 1, **1**, 87 (1993) (in Russian).
[2] S.V. Siparov. Izv. Vyssh. Uchebn. Zaved. Aviats. Tekh., **1**, 84 (1991) (in Russian).
[3] A.N. Volodko, A.Ya. Serov, Mechanics Solids, **1** 10 (1988).
[4] A.N. Sviridenko. Nauchn. Vestn. Mosk. Gos. Tekh. Univ. Grazhdanskoi Aviats. Ser. Aeromekh. Prochn., **111**, 129 (2007) (in Russian).
[5] V.B. Kozlovskii, S.A. Parshentsev, V.V Efimov. *Vertolet s gruzom na vneshnei podveske* (Mashinostroenie, Mashinostroenie-Polet, M., 2008) (in Russian)
[6] V.V. Efimov. Nauchn. Vestn. Mosk. Gos. Tekh. Univ. Grazhdanskoi Aviats. Ser. Aeromekh. Prochn., **111**, 121 (2007) (in Russian).
[7] V.V. Efimov, K.O. Chernigin, Yu.A. Bykov. Nauchn. Vestn. Mosk. Gos. Tekh. Univ. Grazhdanskoi Aviats., **172**, 67 (2011) (in Russian).
[8] A.N. Ryabinin. Vestn. S.-Peterb. Univ. Ser. 1, **2**, 71 (1997) (in Russian).
[9] O. Ivanov, V. Vedeneev. J. Fluids and Structures, **107**, 103393 (2021). DOI: 10.1016/j.jfluidstructs.2021.103393
[10] O. Ivanov, V. Vedeneev. Proceed. ASME. 2021 Pressure Vessels and Piping Conference, PVP 2021 V003T04A020. (2021). DOI: 10.1115/PVP2021-62812
[11] M. Demenkov. AIP Conference Proceedings, **1959**, 050008 (2018) DOI: /10.1063/1.5034636
[12] M.N. Demenkov. In: *XIII Vserossiiskoe soveshchanie po problemam upravleniya VSPU-2019,* Ed. by D.A. Novikov (Inst. Probl. Upravl. Ross. Akad. Nauk, M., 2019), p. 176 (in Russian) DOI: 10.25728/vspu.2019.0176
[13] D. Škrlec, V. Šimović, A. Pender. *2022 45th Jubilee International Convention on Information, Communication and Electronic Technology (MIPRO)* (Opatija, Croatia, 2022), p. 1522. DOI: 10.23919/MIPRO55190.2022.9803322
[14] J.E. Rico, K. Turkoglu. AIAA, **2016-0946** (2016). DOI: 10.2514/6.2016-0946
[15] M.A. Kovalev. Uch. Zap. Leningr. Univ., **7**, 61 (1939) (in Russian).
[16] GOST 20058-80 *Aircraft Dynamics in Atmosphere. Terms, Definitions and Symbols* (Gosstandart, M., 1981) (in Russian)
[17] N.N. Polyakhov, S.A. Zegzhda, M.P. Yushkov. *Teoreticheskaya mekhanika*: uchebnik dlya akademicheskogo bakalavriata (Yurait, M., 2016) (in Russian)
[18] A.N. Ryabinin, N.A. Kiselev. Vestn. S.-Peterb. Univ. Ser. 1. Mat. Mekh. Astron., **3** (61), 315 (2016) (in Russian). DOI: 10.21638/11701/spbu01.2016.216
[19] G.K. Ananda, P.P. Sukumar, M.S. Selig. Aerospace Sc. Technol., **42**, 392 (2015). http://dx.doi.org/10.10.16/j.ast.2014.11.016

Translated by D.Safin